



## Electrochemical Properties of Nonstoichiometric $\text{LiNi}_{0.5}\text{Mn}_{1.5}\text{O}_{4-\delta}$ Thin-Film Electrodes Prepared by Pulsed Laser Deposition

H. Xia,<sup>a</sup> Y. S. Meng,<sup>b,\*</sup> L. Lu,<sup>a,c</sup> and G. Ceder<sup>a,b,\*</sup>

<sup>a</sup>Advanced Materials for Micro- and Nano-System, Singapore-MIT Alliance, Singapore 117576, Singapore

<sup>b</sup>Department of Materials Science and Engineering, Massachusetts Institute of Technology, Cambridge, Massachusetts 02139, USA

<sup>c</sup>Department of Mechanical Engineering, National University of Singapore, Singapore 117576, Singapore

Well-crystallized nonstoichiometric  $\text{LiNi}_{0.5}\text{Mn}_{1.5}\text{O}_{4-\delta}$  thin-film electrodes were prepared by pulsed laser deposition (PLD). The charge/discharge behavior of the nonstoichiometric  $\text{LiNi}_{0.5}\text{Mn}_{1.5}\text{O}_{4-\delta}$  thin film is consistent with the film having a disordered spinel structure with space group  $Fd\bar{3}m$ . These thin-film electrodes exhibit excellent cycle performance and rate capability. The measured Li diffusivity in the film is in the range of  $10^{-12}$  to  $10^{-10}$   $\text{cm}^2/\text{s}$ , which is comparable to that of layered  $\text{LiCoO}_2$ . First principles calculations on the stoichiometric (ordered) spinel  $\text{LiNi}_{0.5}\text{Mn}_{1.5}\text{O}_4$  find no intermediate ordered phases between  $\text{LiNi}_{0.5}\text{Mn}_{1.5}\text{O}_4$  and  $\text{Li}_0\text{Ni}_{0.5}\text{Mn}_{1.5}\text{O}_4$ , leading us to speculate that voltage steps observed in experiments are caused by Ni-Mn disorder, which facilitates Li/vacancy ordering. The presence of a smaller step in "ordered"  $\text{LiNi}_{0.5}\text{Mn}_{1.5}\text{O}_4$  than in disordered  $\text{LiNi}_{0.5}\text{Mn}_{1.5}\text{O}_4$  is consistent with the calculation and may indicate presence of partial disorder even in ordered material. Although a maximum was found for the chemical diffusion coefficient of Li in  $\text{Li}_x\text{Ni}_{0.5}\text{Mn}_{1.5}\text{O}_{4-\delta}$  near  $x = 0.5$ , the self-diffusion coefficient exhibits a minimum at that composition.

© 2007 The Electrochemical Society. [DOI: 10.1149/1.2741157] All rights reserved.

Manuscript submitted January 31, 2007; revised manuscript received March 21, 2007. Available electronically May 31, 2007.

The development of cathode materials for lithium batteries that provide high energy density at fast discharge rates is important to meet the demands for high-power applications such as hybrid electric vehicles and power tools. Among possible cathode materials,  $\text{LiMn}_2\text{O}_4$  with the spinel structure has gained much attention because of its low cost, low toxicity, and reasonably high energy density.<sup>1-3</sup> Several research groups have reported transition metal substituted spinel materials ( $\text{LiM}_x\text{Mn}_{2-x}\text{O}_4$ , M = Ni, Co, Cu, Cr, Fe, etc.) with high working voltages around 5 V.<sup>4-8</sup> Among them,  $\text{LiNi}_{0.5}\text{Mn}_{1.5}\text{O}_4$  is particularly interesting due to its high capacity, good cycle performance, and good rate capability.<sup>9,10</sup> This spinel is fundamentally different from pure Mn spinels as all redox activity takes place on Ni with Mn remaining in the 4+ state. Previous work has shown that  $\text{Mn}^{4+}$ -containing compounds are remarkably stable.<sup>11-13</sup> While nonstoichiometric  $\text{LiNi}_{0.5}\text{Mn}_{1.5}\text{O}_{4-\delta}$  has the normal face-centered spinel ( $Fd\bar{3}m$ ) symmetry with Ni and Mn disordered,  $\text{Mn}^{4+}$  and  $\text{Ni}^{2+}$  ions order in stoichiometric  $\text{LiNi}_{0.5}\text{Mn}_{1.5}\text{O}_4$  resulting in the  $P4_332$  symmetry.<sup>14,15</sup> The disordered  $Fd\bar{3}m$  spinel was found to have superior rate capability to the ordered spinel.<sup>15-17</sup>

In this paper, we report on a study of the structure and electrochemical performance of thin-film  $\text{LiNi}_{0.5}\text{Mn}_{1.5}\text{O}_4$  electrodes deposited by pulsed laser deposition (PLD). Without the presence of polymer binder and carbonaceous powders, thin-film electrodes are ideal samples for studying the intrinsic properties of electrode materials such as its Li diffusivity. Thin-film electrodes can be prepared with various techniques, including radio-frequency sputtering,<sup>18,19</sup> PLD,<sup>20,21</sup> chemical vapor deposition,<sup>22</sup> spin coating,<sup>23</sup> and electrostatic spray deposition.<sup>24,25</sup> Among these, PLD is a powerful and flexible method for fabricating simple and complex metal oxide films, and has several advantages for thin film deposition, including direct stoichiometry transfer from the target to the growing film, high deposition rate and inherent simplicity for the growth of multilayered structures, and easy deposition of dense, textured films with in situ substrate heating.

In this work, nonstoichiometric  $\text{LiNi}_{0.5}\text{Mn}_{1.5}\text{O}_{4-\delta}$  thin films were deposited on stainless steel (SS) and  $\text{SiO}_2/\text{Si}$  (SOS) substrates by PLD. The microstructure and surface morphology of the films were characterized by X-ray diffraction (XRD) and field-emission scan-

ning electron microscopy (FESEM). The crack-free and well-crystallized  $\text{LiNi}_{0.5}\text{Mn}_{1.5}\text{O}_{4-\delta}$  thin films were used to study charge/discharge behavior, cycle performance, rate capability, and Li diffusion in the material. To better rationalize the experimental results, we also carried out first principles computations to examine the voltage and lattice parameters as a function of Li content.

### Experimental

The  $\text{LiNi}_{0.5}\text{Mn}_{1.5}\text{O}_{4-\delta}$  thin films were deposited on SS and  $\text{SiO}_2/\text{Si}$  (SOS) substrates by PLD in a vacuum chamber at a base pressure less than  $10^{-5}$  Torr. The targets for PLD were prepared by synthesizing a mixture of  $\text{MnO}_2$  99.9% (Alfa Aesar), NiO 99% (Alfa Aesar), and LiOH 98% (Merck) at 750°C in air for 24 h. The target-substrate distance was kept at 35 mm. A Lambda Physik KrF excimer laser with wavelength 248 nm was used in the deposition. Laser fluence and repetition rate were controlled at 2 J  $\text{cm}^{-2}$  and at 10 Hz, respectively. Film depositions were carried out at a substrate temperature of 600°C and in an oxygen partial pressure of 200 mTorr for 40 min. All characterization and electrochemical measurements were performed on the films grown on the SS substrates. Thin films on the SOS substrates were only used for estimating the growth rate and thickness of the film.

The structure and crystallinity of the films were investigated using a Shimadzu XRD-6000 X-ray diffractometer with Cu K $\alpha$  radiation. Data was collected in the range of 10–70° at a scan rate of 2°/min. Surface morphology and roughness of thin films were characterized using a Hitachi S-4100 FESEM. The cross sections of thin films on SOS substrates were observed by FESEM to estimate the thin film thickness and the growth rate.

Electrochemical experiments were conducted using a Solartron 1287 cell test system. The Swagelok type cells consist of a Li-metal foil counter electrode, a  $\text{LiNi}_{0.5}\text{Mn}_{1.5}\text{O}_{4-\delta}$  thin-film working electrode with an active area of approximately 0.785  $\text{cm}^2$ , and 1 M LiPF<sub>6</sub> in EC/DEC (1/1 vol %) as the electrolyte. Galvanostatic charge/discharge measurements were carried out in the voltage range between 3 and 5 V with a constant current density (10–1000  $\mu\text{A}/\text{cm}^2$ ). Cyclic voltammogram (CV) measurements were carried out in the voltage range between 3.5 and 5 V with a scan rate of 0.2 mV/s. To measure the chemical diffusion coefficient, the potentiostatic intermittent titration technique (PITT) was used with a potential step of 10 mV. The potential was stepped to the next level when the current dropped below 0.1  $\mu\text{A}/\text{cm}^2$ . This procedure was repeated between 4.50 and 4.90 V for both increas-

\* Electrochemical Society Active Member.

<sup>z</sup> E-mail: ysmeng@mit.edu

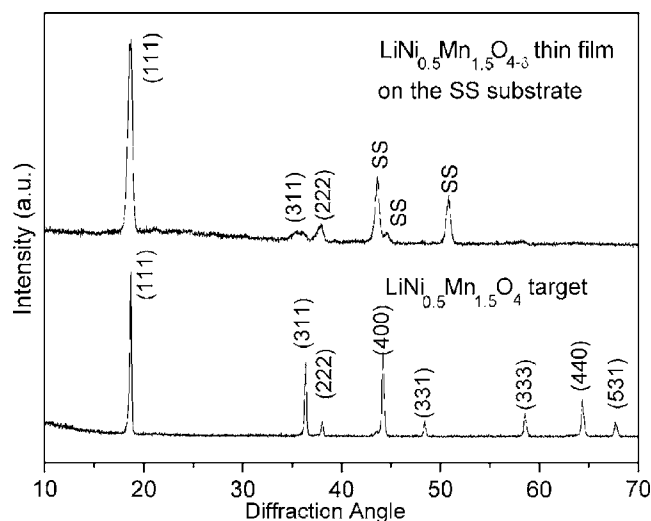


**Figure 1.** XRD spectra of the  $\text{LiNi}_{0.5}\text{Mn}_{1.5}\text{O}_4$  target and the PLD  $\text{LiNi}_{0.5}\text{Mn}_{1.5}\text{O}_{4-\delta}$  film (substrate peaks are marked as SS).

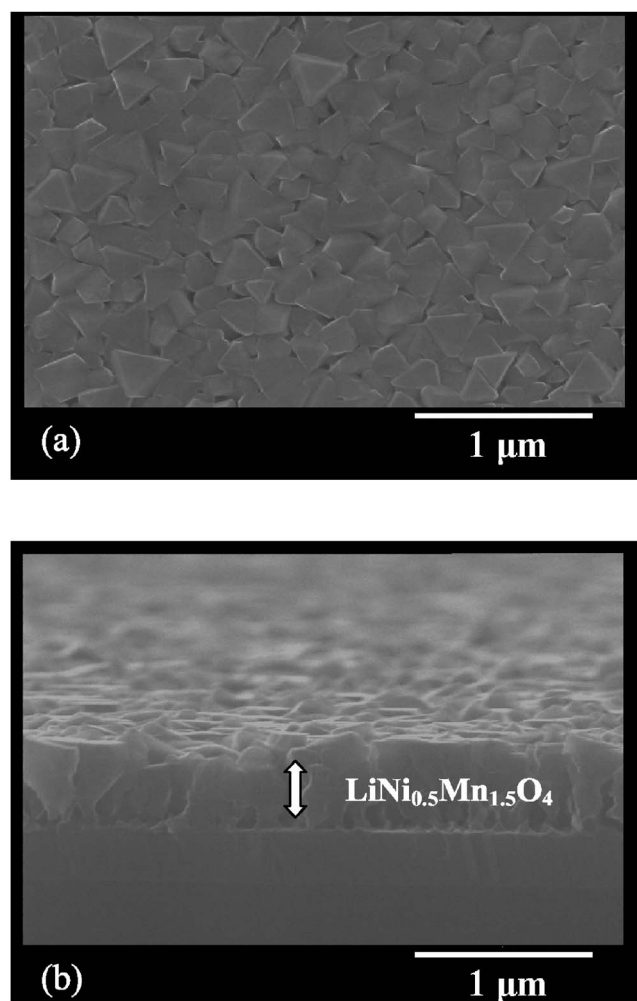
ing and decreasing potentials. The diffusivity was extracted from the current response using a standard Cottrell analysis.<sup>26</sup>

**Computational method.**— All first principles energies were calculated with the spin-polarized generalized gradient approximation to density functional theory using the projector-augmented wave method<sup>27</sup> as implemented in the Vienna ab initio simulation package (VASP).<sup>28</sup> A plane-wave basis with a kinetic energy cutoff of 370 eV was used. A reciprocal-space  $k$ -point grid of  $5 \times 5 \times 5$  was used. Structures were fully relaxed. The  $+U$  correction term in the Dudarev scheme<sup>29</sup> was used with  $U = 5.96$  eV for Ni and  $U = 5$  eV for Mn. This  $+U$  scheme corrects for the self-interaction in the transition-metal  $d$  orbitals and has been shown to improve the prediction of voltages<sup>30</sup> and phase stability.<sup>31</sup> Voltages were calculated as averages between a Li content of zero and one per formula unit with the equations outlined in Ref. 32.

## Results

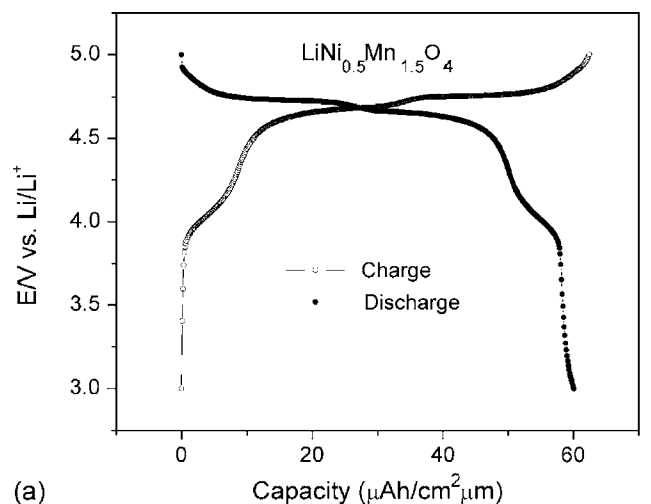
**Microstructure and surface morphology.**— In a previous paper,<sup>33</sup> we showed that  $\text{LiNi}_{0.5}\text{Mn}_{1.5}\text{O}_4$  thin films deposited by PLD always have a small amount of oxygen deficiency as a result of oxygen loss during the high-vacuum deposition. We therefore write the molecular formula of the film as  $\text{LiNi}_{0.5}\text{Mn}_{1.5}\text{O}_{4-\delta}$ . The XRD spectra of the  $\text{LiNi}_{0.5}\text{Mn}_{1.5}\text{O}_4$  target and the  $\text{LiNi}_{0.5}\text{Mn}_{1.5}\text{O}_{4-\delta}$  film on the SS substrate are shown in Fig. 1. The XRD spectrum indicates that the target is single phase  $\text{LiNi}_{0.5}\text{Mn}_{1.5}\text{O}_4$ . The Miller index for each peak was determined based on a spinel structure with  $Fd\bar{3}m$  space group. The diffraction peaks of the  $\text{LiNi}_{0.5}\text{Mn}_{1.5}\text{O}_{4-\delta}$  film can be indexed based on the XRD spectrum of the target. Only three diffraction peaks from the film are observed and indexed as (111), (311), and (222). The (111) peak is very sharp and has high intensity, indicating that the film has a high degree of crystallinity and a strong (111) texture. Because only a few diffraction peaks are visible we cannot determine if the spinel film has space group  $Fd\bar{3}m$  or  $P4_332$ .

Figure 2 shows SEM micrographs of the top view of the  $\text{LiNi}_{0.5}\text{Mn}_{1.5}\text{O}_{4-\delta}$  film on the SS substrate and a cross-sectional view of the  $\text{LiNi}_{0.5}\text{Mn}_{1.5}\text{O}_{4-\delta}$  film on the SOS substrate. The film is composed of well-defined grains and has a very smooth surface without cracks. Most of the grains exhibit octahedral or pseudo-polyhedral forms reflecting the cubic spinel structure. The average grain size is about 200–300 nm. From the cross-sectional view of the film on the SOS substrate, the film thickness is estimated to be about 500 nm.

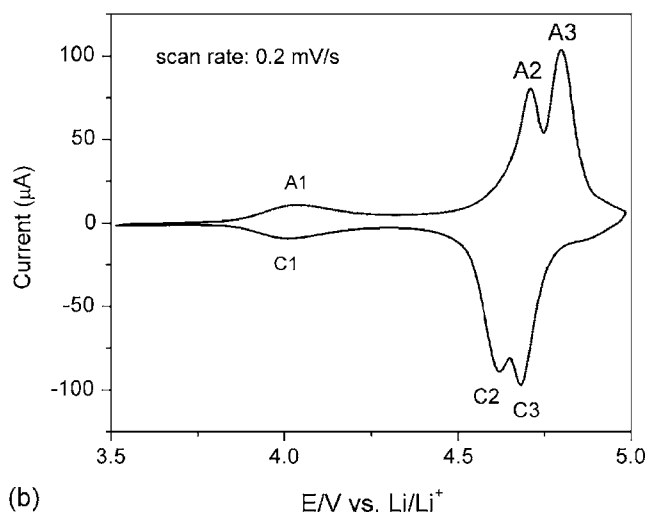


**Figure 2.** SEM micrographs of (a) top view of an  $\text{LiNi}_{0.5}\text{Mn}_{1.5}\text{O}_{4-\delta}$  film on the SS substrate and (b) cross-sectional view of  $\text{LiNi}_{0.5}\text{Mn}_{1.5}\text{O}_{4-\delta}$  film on the SOS substrate.

**Electrochemical behavior.**— Charge/discharge and CV measurements were performed on a  $\text{LiNi}_{0.5}\text{Mn}_{1.5}\text{O}_{4-\delta}/\text{Li}$  cell. Figure 3a shows the typical charge/discharge curves for the PLD  $\text{LiNi}_{0.5}\text{Mn}_{1.5}\text{O}_{4-\delta}$  thin-film electrode cycled between 3 and 5 V with a current of  $20 \mu\text{A}/\text{cm}^2$ . Three voltage plateaus can be observed in both charge and discharge curves and in the CV curves in Fig. 3b. As shown in Fig. 3b, well-resolved reversible peaks are observed at 4.1 (A1), 4.7 (A2), and 4.8 V (A3) on charge, and at 4.0 (C1), 4.6 (C2), and 4.7 V (C3) on discharge. The integrated area of the 4 V peaks is small compared with those of the high voltage peaks around 4.7 V. This electrochemical behavior is similar to what has been observed for composite electrodes.<sup>6,9</sup>  $\text{LiNi}_{0.5}\text{Mn}_{1.5}\text{O}_4$  powders used in composite electrodes can lose oxygen and/or form NiO or  $\text{Li}_x\text{Ni}_{1-x}\text{O}$  impurity phases during high-temperature calcination. The resulting  $\text{Mn}^{3+}$  formed leads to the appearance of the 4 V plateau.<sup>6</sup> The small amount of  $\text{Mn}^{3+}$  in the PLD film is probably induced by oxygen loss during the vacuum deposition. For stoichiometric  $\text{LiNi}_{0.5}\text{Mn}_{1.5}\text{O}_4$ , all Ni exist in the 2+ oxidation state and all Mn exist in the 4+ oxidation state, resulting in the absence of the 4 V potential plateau.<sup>15</sup> The two major peaks between 4.5 and 5 V for both charge and discharge may correspond to distinct redox voltages for  $\text{Ni}^{2+}/\text{Ni}^{3+}$  and  $\text{Ni}^{3+}/\text{Ni}^{4+}$ , or be due to ordering of Li and vacancies at  $x = 0.5$  in  $\text{Li}_x\text{Ni}_{0.5}\text{Mn}_{1.5}\text{O}_4$ , as has been predicted theoretically for other spinels.<sup>34,35</sup> The hypothesis of separate  $\text{Ni}^{2+}/\text{Ni}^{3+}$  and  $\text{Ni}^{3+}/\text{Ni}^{4+}$  redox couples was put forward by Terada et al.<sup>36</sup> based on



(a)



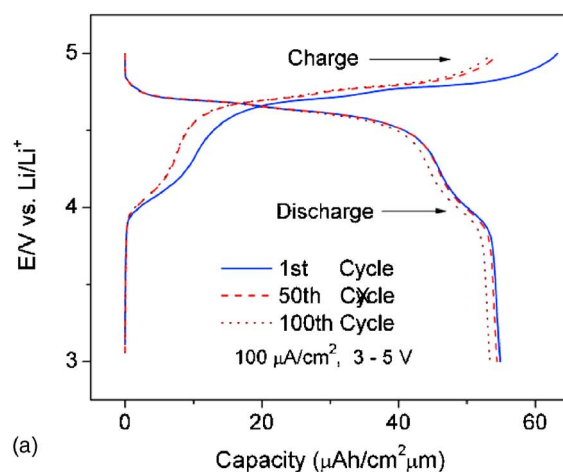
(b)

**Figure 3.** (a) Typical charge/discharge curves for the PLD  $\text{LiNi}_{0.5}\text{Mn}_{1.5}\text{O}_{4-\delta}$  thin film on the SS substrate cycled between 3 and 5 V with a current of  $20 \mu\text{A}/\text{cm}^2$ . (b) Cyclic voltammogram of a  $0.5 \mu\text{m}$  thick  $\text{LiNi}_{0.5}\text{Mn}_{1.5}\text{O}_{4-\delta}$  thin film electrode cycled between 3.5 and 5 V vs  $\text{Li}/\text{Li}^+$  at  $0.2 \text{ mV}/\text{s}$  scan rate.

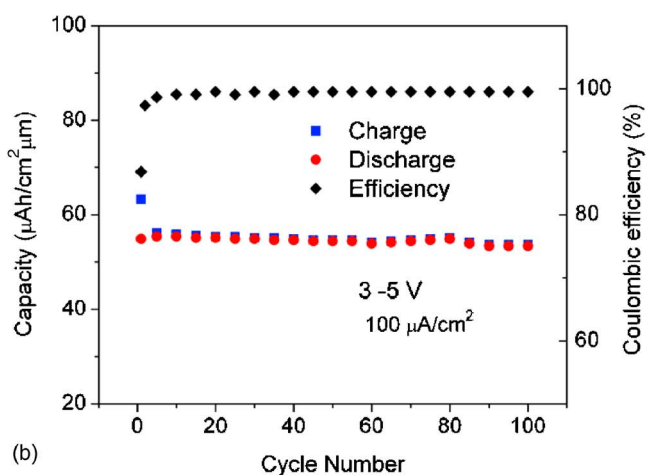
in situ X-ray absorption fine structure measurements, and by Dokko et al.<sup>37</sup> based on in situ Raman spectroscopic measurements.

**Cycle performance.**— The  $\text{Li}/\text{LiNi}_{0.5}\text{Mn}_{1.5}\text{O}_{4-\delta}$  cell with a thin-film electrode was cycled between 3 and 5 V at a current of  $100 \mu\text{A}/\text{cm}^2$  for 100 cycles. The 1st, 50th, and 100th, charge/discharge curves are shown in Fig. 4a. Except for the first cycle, the charge/discharge capacities are highly reversible, indicating that the  $\text{LiNi}_{0.5}\text{Mn}_{1.5}\text{O}_{4-\delta}$  in the film exhibits good structural stability. The 100th discharge curve almost overlaps with the first discharge curve except for a very small capacity loss. As shown in Fig. 4b, the PLD  $\text{LiNi}_{0.5}\text{Mn}_{1.5}\text{O}_{4-\delta}$  thin film exhibits excellent capacity retention and high coulombic efficiency. After 100 cycles, the thin-film electrode still delivers 97.3% of its initial discharge capacity, corresponding to a capacity fade of 0.026% per cycle. At a current of  $100 \mu\text{A}/\text{cm}^2$  (corresponding to a 3 C rate), the specific capacity of a  $\text{LiNi}_{0.5}\text{Mn}_{1.5}\text{O}_{4-\delta}$  thin-film electrodes is around  $55 \mu\text{Ah}/\text{cm}^2 \mu\text{m}$ , which is comparable to the best results reported in the literature for  $\text{LiMn}_2\text{O}_4$  and  $\text{LiCoO}_2$  thin-film electrodes under similar rate.<sup>38-42</sup>

**Rate capability.**— Figure 5a shows the discharge curves of the PLD  $\text{LiNi}_{0.5}\text{Mn}_{1.5}\text{O}_{4-\delta}$  thin film between 3 and 5 V measured at current densities varying from 10 to  $1000 \mu\text{A}/\text{cm}^2$ . The discharge



(a)



(b)

**Figure 4.** (Color online) (a) The 1st, 50th, and 100th charge/discharge curves of the  $\text{Li}/\text{LiNi}_{0.5}\text{Mn}_{1.5}\text{O}_{4-\delta}$  cell cycled between 3 and 5 V with a current of  $100 \mu\text{A}/\text{cm}^2$  for 100 cycles. (b) Cycle performance of the  $\text{Li}/\text{LiNi}_{0.5}\text{Mn}_{1.5}\text{O}_{4-\delta}$  cell cycled between 3 and 5 V with a current of  $100 \mu\text{A}/\text{cm}^2$ .

capacity at a low current density of  $10 \mu\text{A}/\text{cm}^2$  can reach  $60 \mu\text{Ah}/\text{cm}^2 \mu\text{m}$ . As the current density increases from 10 to  $100 \mu\text{A}/\text{cm}^2$ , there is only a very small loss of discharge capacity. Increasing the current density further from 100 to  $1000 \mu\text{A}/\text{cm}^2$  leads to a lowering of the voltage and capacity loss. Figure 5b shows the relative discharge capacities at different current densities normalized by the discharge capacity at  $10 \mu\text{A}/\text{cm}^2$ . It is clear that the discharge capacity profile can be divided into two regions. When the charge/discharge rate is less than  $100 \mu\text{A}/\text{cm}^2$ , only a very small capacity loss is observed, indicating nearly complete lithium insertion into the film. When the charge/discharge rate is higher than  $100 \mu\text{A}/\text{cm}^2$ , a significant capacity loss is observed. Under these conditions, the discharge voltage drops substantially with the current density. At the current density of  $100 \mu\text{A}/\text{cm}^2$  corresponding to a 3 C rate for the cell, about 94% of the full capacity is maintained. Park and Sun et al.<sup>10</sup> have reported that a composite electrode of  $\text{LiNi}_{0.5}\text{Mn}_{1.5}\text{O}_4$  ( $P4_332$ ) can reach up to 92% of its full capacity at a 2 C rate.

**Li diffusion.**— The rate capability results indicate excellent Li diffusion in the  $\text{LiNi}_{0.5}\text{Mn}_{1.5}\text{O}_{4-\delta}$  film. With increasing interest in high power density, the kinetics of Li diffusion in insertion electrodes has become an important research topic.<sup>43-47</sup> Kinetics studies on Li diffusion in  $\text{LiNi}_{0.5}\text{Mn}_{1.5}\text{O}_4$  are quite limited.<sup>48,49</sup> Thin-film electrodes are ideal candidates for diffusion measurements because

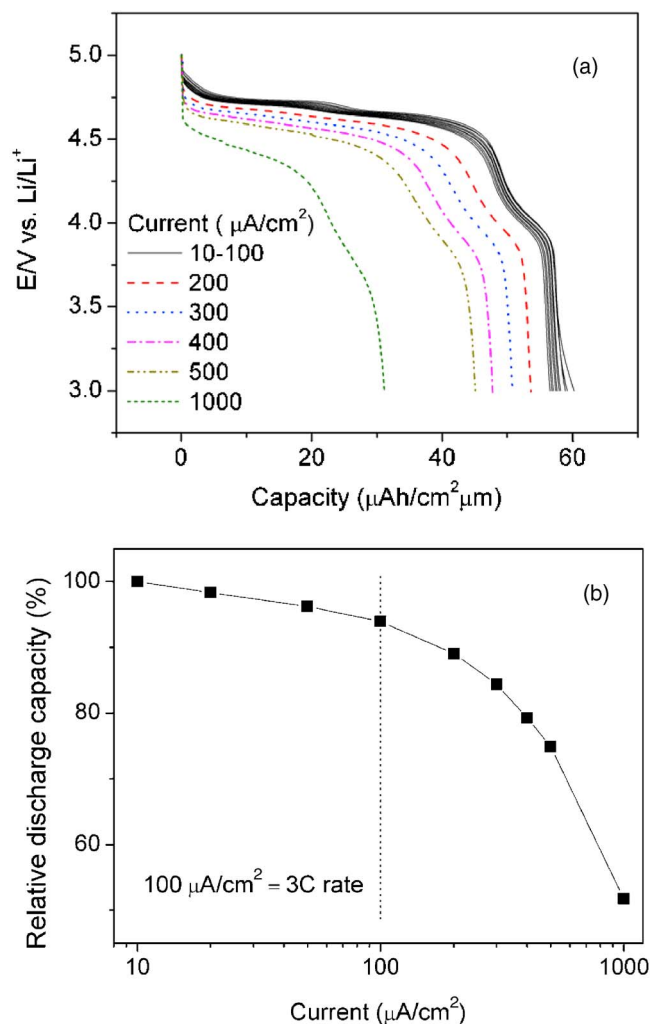


**Figure 5.** (Color online) (a) Discharge curves of the  $\text{LiNi}_{0.5}\text{Mn}_{1.5}\text{O}_{4-\delta}$  thin-film electrode measured at different current densities between 3 and 5 V. (b) Rate capability of the  $\text{LiNi}_{0.5}\text{Mn}_{1.5}\text{O}_{4-\delta}$  thin-film electrode. (The discharge capacities at different current densities were normalized by the discharge capacity obtained at  $10 \mu\text{A}/\text{cm}^2$ ).

their well-defined geometries of pure active materials can facilitate access to the intrinsic properties of the active materials. We use the PITT method to study the Li diffusion in the PLD  $\text{LiNi}_{0.5}\text{Mn}_{1.5}\text{O}_{4-\delta}$  thin-film electrode. In PITT the current response to a potential step is measured. The diffusion coefficient can be extracted from the current response assuming a standard Cottrell solution for the lithium flux at the surface. A detailed explanation of the PITT method can be found in Ref. 26. Figure 6 shows the chemical diffusion coefficient  $\tilde{D}_{\text{Li}}$  of the  $\text{LiNi}_{0.5}\text{Mn}_{1.5}\text{O}_{4-\delta}$  film as a function of potential vs  $\text{Li}/\text{Li}^+$ . In the potential range between 4.5 and 4.9 V, the chemical diffusion coefficient of Li varies from  $10^{-12}$  to  $10^{-10} \text{ cm}^2/\text{s}$ . The values of  $\tilde{D}_{\text{Li}}$  from our results are 1–2 orders of magnitude higher than those obtained by Kovacheva et al.<sup>48</sup> on composite electrodes but agree well with those obtained with electrochemical impedance spectroscopy (EIS) on electrostatically sprayed films.<sup>49</sup> The difference in  $\tilde{D}_{\text{Li}}$  between composite electrodes and thin-film electrodes is probably attributed to different assumptions for the geometrical factors. Because thin-film electrodes have better-defined geometry, their  $\tilde{D}_{\text{Li}}$  values are probably more reliable.

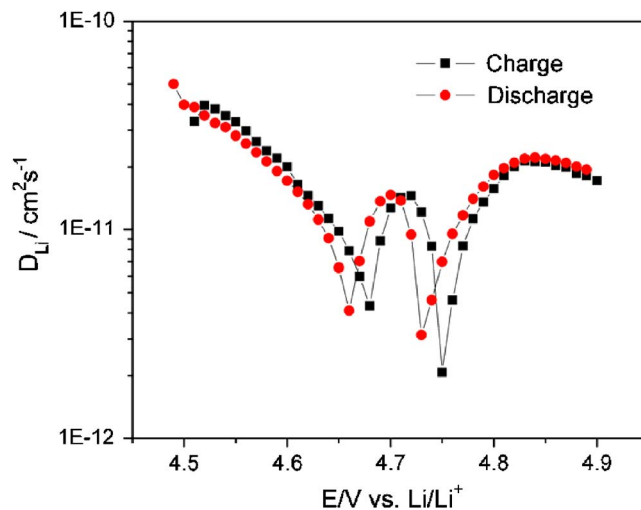


**Figure 6.** (Color online) Chemical diffusion coefficient of Li in an  $\text{LiNi}_{0.5}\text{Mn}_{1.5}\text{O}_{4-\delta}$  thin film obtained as a function of potential by PITT.

### Discussion

Previous studies on  $\text{LiNi}_{0.5}\text{Mn}_{1.5}\text{O}_4$  composite electrodes have found a symmetry of either  $Fd\bar{3}m$  or  $P4_332$  for the crystal structure, depending on the synthesis processes.<sup>15,17</sup> The  $Fd\bar{3}m$  structure is typically found in off-stoichiometric  $\text{LiNi}_{0.5}\text{Mn}_{1.5}\text{O}_{4-\delta}$  prepared by a direct high-temperature calcination process. It has been reported that additional annealing at  $700^\circ\text{C}$  can lead to stoichiometric  $\text{LiNi}_{0.5}\text{Mn}_{1.5}\text{O}_4$  with symmetry  $P4_332$ .<sup>50</sup> In the spinel structure, the oxygen ions at the 32(e) sites form a cubic-close packed lattice with the cations occupying the tetrahedral and octahedral interstices. The tetrahedral 8(a) sites are usually occupied by lithium ions. In the  $Fd\bar{3}m$  space group, Ni and Mn atoms are randomly distributed on the 16(d) sites but cation ordering at the octahedral 16(d) sites leads to the  $P4_332$  space group, as discussed by Strobel,<sup>51</sup> Kim,<sup>15</sup> and Ariyoshi<sup>52</sup> et al. The difference between  $Fd\bar{3}m$  and  $P4_332$  symmetry cannot be resolved in the XRD of the thin film due to the limited number of diffraction peaks visible, but some indication may be found in the electrochemical signal of the film. It has been observed that the stoichiometric  $\text{LiNi}_{0.5}\text{Mn}_{1.5}\text{O}_4$  exhibits a flat voltage profile near 4.7 V and no plateau at 4 V, while nonstoichiometric  $\text{LiNi}_{0.5}\text{Mn}_{1.5}\text{O}_{4-\delta}$  exhibits a stepwise voltage profile near 4.7 V and a small plateau in the 4 V region.<sup>15,52</sup> Based on this comparison the charge/discharge behavior (Fig. 3a) of our thin-film electrode would indicate that the film is nonstoichiometric  $\text{LiNi}_{0.5}\text{Mn}_{1.5}\text{O}_{4-\delta}$  with  $Fd\bar{3}m$  symmetry. Several investigations have found that disordered  $\text{LiNi}_{0.5}\text{Mn}_{1.5}\text{O}_{4-\delta}$  exhibits better rate capability than ordered  $\text{LiNi}_{0.5}\text{Mn}_{1.5}\text{O}_4$ .<sup>15,53</sup> The PLD film exhibits good rate capability and its electrochemical properties agree well with those of the composite electrode of the disordered  $\text{LiNi}_{0.5}\text{Mn}_{1.5}\text{O}_{4-\delta}$ , which we take as further indication that Ni and Mn are disordered in the film.

The voltage profiles of Li concentration in the  $\text{Li}_x\text{Ni}_{0.5}\text{Mn}_{1.5}\text{O}_{4-\delta}$  thin film are shown in Fig. 7. Three potential regions can be clearly distinguished:  $x > 0.85$  (region 1),  $0.5 < x < 0.85$  (region 2), and  $x < 0.5$  (region 3). In the 4 V region Li removal is accompanied by oxidation of  $\text{Mn}^{3+}$  to  $\text{Mn}^{4+}$ . In region 2, the voltage curve shows a quasi-plateau increasing gradually with decreasing  $x$ . Such gradual voltage increase may indicate a solid solution state, consistent with the absence of any phase transition in ex situ<sup>15</sup> and in situ<sup>53</sup> XRD results on disordered ( $Fd\bar{3}m$ )  $\text{Li}_x\text{Ni}_{0.5}\text{Mn}_{1.5}\text{O}_{4-\delta}$ . In region 3, the voltage curve is flat between  $\sim 0.2 < x < \sim 0.4$ , indicating a two-phase reaction. This is in agreement with the ex situ XRD result by Kim et al.<sup>15</sup> who found

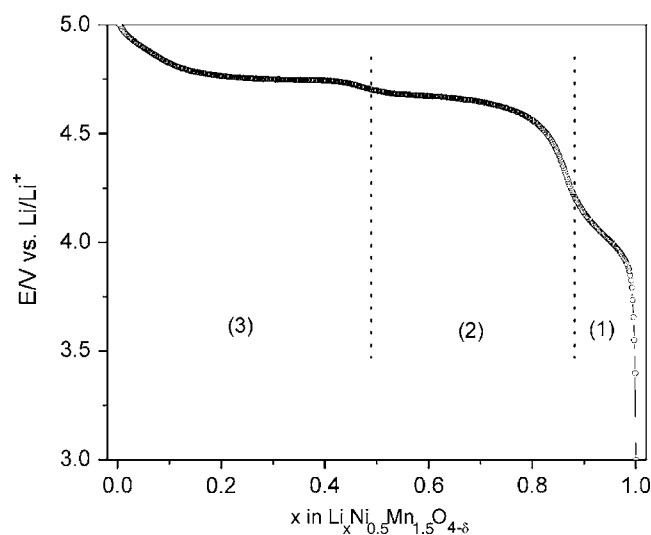


**Figure 7.** The first charge curve for  $\text{Li}_x\text{Ni}_{0.5}\text{Mn}_{1.5}\text{O}_{4-\delta}$  as a function of Li concentration at a slow current rate of  $10 \mu\text{A}/\text{cm}^2$ .

a phase transition when  $x < 0.5$  for the disordered  $\text{Li}_x\text{Ni}_{0.5}\text{Mn}_{1.5}\text{O}_{4-\delta}$ . The sudden jump of the potential around  $x = 0.5$  in Fig. 7, is similar to the electrochemical behavior of spinel  $\text{LiMn}_2\text{O}_4$  where Gao et al.<sup>54</sup> attributed the step to ordering of Li and vacancies. Van der Ven et al.<sup>55</sup> and Amundsen et al.<sup>56</sup> supported this idea of ordering using, respectively, ab initio results and spectroscopic methods. Recently, Kashiwagi et al.<sup>57</sup> further proved this idea by measuring the reaction entropy. They attributed the change in the sign in reaction entropy near  $x \sim 0.5$  to the ordered arrangement of Li/vacancies. Because the average structure of nonstoichiometric  $\text{LiNi}_{0.5}\text{Mn}_{1.5}\text{O}_{4-\delta}$  is the same as that of  $\text{LiMn}_2\text{O}_4$ , Li/vacancy ordering in the former seems plausible. Using in situ XRD Kunduraci et al.<sup>53</sup> additionally observed broadening of the XRD peaks and small plateaus in the lattice parameter progression around  $x = 0.5$ . They attributed this phenomenon to the presence of a short, poorly defined, two-phase region. Therefore, the broadening of the XRD peaks at about  $x = 0.5$  observed by Kunduraci et al.<sup>53</sup> is probably due to the order/disorder transitions at about  $x = 0.5$ . Several investigations have found that the step at  $x = 0.5$  is larger for the disordered spinel than for the ordered spinel.<sup>14,15</sup> We speculate that the ordering arrangement of Ni and Mn in the ordered spinel is probably not commensurate with the preferred Li/vacancy ordering at  $x = 0.5$  so that ordering of Ni and Mn suppresses Li/vacancy ordering.

It is difficult to study disordered systems by first principles methods,<sup>58</sup> and we investigated instead the ordered spinel ( $P4_332$ ). Although the transition metal ions are ordered in the calculation, the exact arrangement of Ni/Mn only influences the lattice parameters and average voltage by a small amount.<sup>15,52</sup> The calculated lattice parameter and average voltage are shown in Table I. Although the GGA + U approach overestimates the absolute values of the lattice

parameters, the calculated changes in the lattice parameters upon delithiation match well with experimental values. The calculated change in lattice parameter from fully lithiated  $\text{LiNi}_{0.5}\text{Mn}_{1.5}\text{O}_4$  to fully delithiated  $\text{Li}_0\text{Ni}_{0.5}\text{Mn}_{1.5}\text{O}_4$  is only 1.4% (1.8% from experimental measurement<sup>52</sup>). This small structure change during the Li insertion/extraction may contribute to the excellent cyclability of this material. As shown in Table I, the average voltage for the entire lithium composition is calculated to be 4.712 V, which is in close agreement with the experimental value of 4.729 V.<sup>52</sup> This indicates that the choice of U values in our DFT + U approach for Ni and Mn are appropriate. We investigated whether stable configurations existed for  $\text{LiNi}_{0.5}\text{Mn}_{1.5}\text{O}_4$ , but found none that are stable against phase separation into  $\text{Li}_0\text{Ni}_{0.5}\text{Mn}_{1.5}\text{O}_4$  and  $\text{LiNi}_{0.5}\text{Mn}_{1.5}\text{O}_4$ . The energy of the lowest energy configuration at  $\text{LiNi}_{0.5}\text{Mn}_{1.5}\text{O}_4$  is +50 meV/FU (one FU consists of four oxygens) above the phase separated state. Hence, we predict that in a fully ordered material Li extraction would proceed through a two-phase reaction or solid solution with no steps at intermediate compositions. In experiments, a very small voltage step is observed at  $\text{Li}_{0.5}\text{Ni}_{0.5}\text{Mn}_{1.5}\text{O}_4$  for the  $P4_332$  phase and this step increases as the spinel becomes more disordered.<sup>15,52</sup> It is possible that our calculation represent the limit of the perfectly ordered  $P4_332$  structure and that a very small voltage step is present in experiments on  $P4_332$  because of small partial disorder. The appearance of a larger step at  $x = 0.5$  for disordered than for ordered systems seems counterintuitive, as one might expect that Li/vacancy ordering as present in the layered  $\text{LiCo}_2\text{O}_4$ <sup>34</sup> and  $\text{LiMn}_2\text{O}_4$  spinel<sup>35</sup> could more easily occur in an Ni–Mn ordered environment. This argument only applies if the preferred Li/vacancy and Ni/Mn ordering are commensurate. If not, Ni/Mn ordering may actually reduce the ability of Li/vacancy to order. Another possibility which has been put forward on the basis of x-ray absorption fine structure (XAFS)<sup>36</sup> and Raman<sup>37</sup> results is that the step is due to a change in redox couple from  $2+/3+$  to  $3+/4+$ . Both XAFS and Raman experiments were performed on the disordered  $Fd\bar{3}m$  spinel. It is possible that  $\text{Ni}^{3+}$  can form more easily in the random Ni/Mn distribution and not in the ordered Ni/Mn arrangement.

Two mechanisms have been proposed in the literature to explain the superior rate capability of the disordered  $\text{LiNi}_{0.5}\text{Mn}_{1.5}\text{O}_{4-\delta}$  over the ordered  $\text{LiNi}_{0.5}\text{Mn}_{1.5}\text{O}_4$ . Kim et al.<sup>15</sup> attribute the lower rate performance of the ordered  $\text{LiNi}_{0.5}\text{Mn}_{1.5}\text{O}_4$  to the two-phase reactions which causes strain. Disordered  $\text{LiNi}_{0.5}\text{Mn}_{1.5}\text{O}_{4-\delta}$  has larger solid-solution limits for Li and as such the strain between the coexisting phases is less. Though the ordered spinel and the disordered spinel will go through different phase transitions during Li insertion/extraction, the changes of the lattice parameter of these two spinels are small and almost the same.<sup>15,53</sup> Therefore, it is not obvious that strain plays a role in the rate capability. Kunduraci et al.<sup>17,53</sup> on the other hand, recently suggested that the poor rate capability of the ordered  $\text{LiNi}_{0.5}\text{Mn}_{1.5}\text{O}_4$  is due to its lower electronic conductivity. Their result<sup>17</sup> shows that there is a systematic 2.5 orders of magnitude difference between the highest electronic conductivity ( $Fd\bar{3}m$ ) to the lowest conductivity ( $P4_332$ ). They believe that the electron hopping from  $\text{Mn}^{3+}$  to  $\text{Mn}^{4+}$  leads to higher electronic conductivity in disordered spinel.

The chemical diffusion coefficient in the disordered  $\text{LiNi}_{0.5}\text{Mn}_{1.5}\text{O}_{4-\delta}$  thin film shows two minima for both charge and discharge at the potentials where  $V(x)$  is nearly constant (Fig. 6 and 7). If there is a two-phase region, Li transport involves diffusion in two phases coupled to boundary kinetics and a single  $\tilde{D}_{\text{Li}}$  is not meaningful. In the case of our spinel  $\text{LiNi}_{0.5}\text{Mn}_{1.5}\text{O}_{4-\delta}$  thin film with space group of  $Fd\bar{3}m$ , there is probably a two-phase region between two cubic phases occurring when  $x < 0.4$ .<sup>15</sup> Therefore, the  $\tilde{D}_{\text{Li}}$  measured in this two-phase region should only be considered to be an effective chemical diffusion coefficient. It is instructive to separate Li mobility effects from thermodynamic effects by factor-

**Table I.** Comparison of the calculated and experimental values of lattice parameter and average voltages.

	$\text{LiNi}_{1/2}\text{Mn}_{3/2}\text{O}_4$	$\text{Li}_{0.5}\text{Ni}_{1/2}\text{Mn}_{3/2}\text{O}_4$	$\text{Li}_0\text{Ni}_{1/2}\text{Mn}_{3/2}\text{O}_4$
$\alpha_{\text{exp}}$	8.167 Å [52]	8.092 Å [52]	8.005 Å [52]
$\alpha_{\text{cal}}$	8.313 Å	8.278 Å <sup>a</sup>	8.193 Å
$V_{\text{exp}}$		( $0.5 \leq x \leq 1$ ) 4.718 V [52]	
		( $0 \leq x \leq 0.5$ ) 4.739 V [52]	
$V_{\text{cal}}$		( $0 \leq x \leq 1$ ) 4.712 V	

<sup>a</sup> The structure is slightly distorted due to Jahn-Teller active  $\text{Ni}^{3+}$ ; average lattice parameter is calculated.

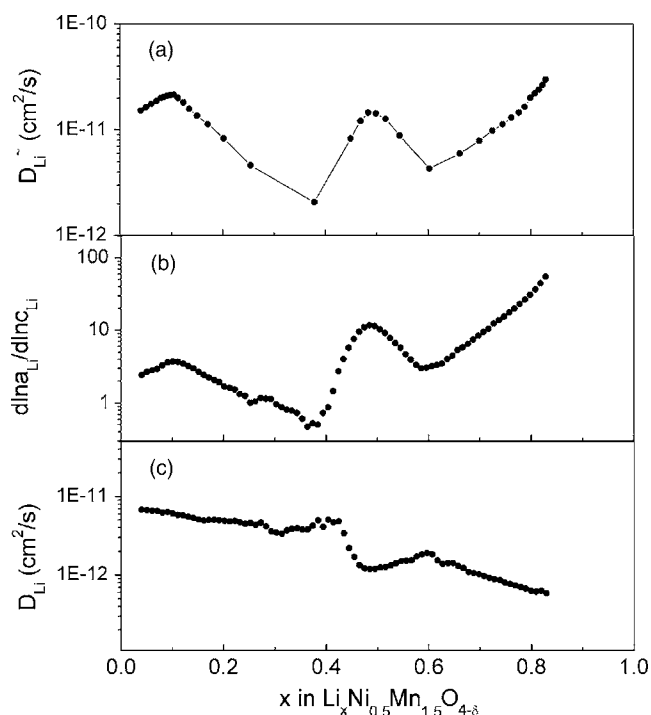


**Figure 8.** Compositional variation of (a) chemical diffusion coefficient of Li, (b) thermodynamic factor of Li, and (c) self-diffusion coefficient of Li obtained by PITT at room temperature using an  $\text{LiNi}_{0.5}\text{Mn}_{1.5}\text{O}_{4-\delta}$  thin-film electrode.

ing the chemical diffusion coefficient ( $\tilde{D}_{\text{Li}}$ ) as the product of the self-diffusion coefficient ( $D_{\text{Li}}$ ) and the thermodynamic factor ( $\Theta$ )<sup>26</sup>

$$\tilde{D}_{\text{Li}} = D_{\text{Li}}\Theta = D_{\text{Li}} \frac{\partial \ln a_{\text{Li}}}{\partial \ln c_{\text{Li}}} \quad [1]$$

where  $a_{\text{Li}}$  is the activity coefficient of Li.  $\Theta$  can be determined independently from the Fig. 7 according to the following expression

$$\Theta = \frac{\partial \ln a_{\text{Li}}}{\partial \ln c_{\text{Li}}} = -\frac{F x dV}{RT dx} \quad [2]$$

In Eq. 2,  $V$  is the voltage,  $R$  is the gas constant,  $F$  is the Faraday's constant, and  $T$  is the absolute temperature.  $\Theta$  obtained from Fig. 7 is shown in Fig. 8b. Note that the  $x$  dependence of  $\Theta$  is similar to that of the  $\tilde{D}_{\text{Li}}$  (Fig. 8a) showing minima at  $x = \sim 0.4$  and  $x = \sim 0.6$ , and one maximum at  $x = \sim 0.5$ . The self diffusion coefficient calculated using Eq. 1 is shown in Fig. 8c. The self-diffusion coefficient represents the Li diffusivity when no gradient of concentration is present and is a better measure of the intrinsic Li mobility than the chemical diffusivity  $\tilde{D}_{\text{Li}}$ . The self-diffusivity,  $D_{\text{Li}}$ , has a minimum near  $x = 0.5$  and two maxima at  $x \approx 0.4$  and  $x \approx 0.6$ , which is quite different from the behavior of  $\tilde{D}_{\text{Li}}$ . The minimum of  $D_{\text{Li}}$  near  $x = 0.5$  indicates a minimum in mobility which is probably caused by the Li/vacancy ordering which binds free vacancies, as discussed by Van der Ven.<sup>59</sup> Because the thermodynamic factor  $\Theta$  usually is maximal near an ordered phase, the chemical diffusivity can be minimal or maximal depending on the relative strength of  $D_{\text{Li}}$  and  $\Theta$ . For our  $\text{LiNi}_{0.5}\text{Mn}_{1.5}\text{O}_{4-\delta}$  thin film, the chemical diffusion coefficient  $\tilde{D}_{\text{Li}}$  shows a maximum at  $x = 0.5$  indicating that the chemical diffusion coefficient is dominated by  $\Theta$ . A similar phenomenon was observed in  $\text{LiCoO}_2$  thin film electrodes.<sup>45</sup>

The Li diffusivity we find for spinel  $\text{LiNi}_{0.5}\text{Mn}_{1.5}\text{O}_4$  is comparable to that of layered  $\text{LiCoO}_2$  ( $10^{-12}$  to  $10^{-10}$   $\text{cm}^2/\text{s}$ ),<sup>43</sup> even though diffusion in both structures occurs along different paths.

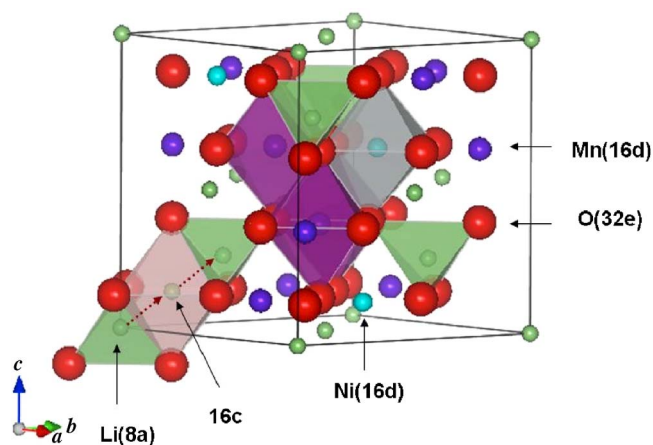


**Figure 9.** (Color online) Diffusion path of lithium in the spinel  $\text{LiNi}_{0.5}\text{Mn}_{1.5}\text{O}_4$  ( $Fd\bar{3}m$ ).

$\text{LiCoO}_2$  has a layered structure with a nearly cubic close-packed arrangement of oxygen ions, and lithium and cobalt ions occupying alternate layers of octahedral sites. In such a structure, Li diffuses two-dimensionally by hopping from octahedral to octahedral site through a tetrahedral site by means of a divacancy mechanism.<sup>59</sup> In spinel  $\text{LiNi}_{0.5}\text{Mn}_{1.5}\text{O}_4$  ( $Fd\bar{3}m$ ) Li diffuses by moving from an 8(a) site to the neighboring empty octahedral 16(c) site, and then to the next 8(a) site. The 8a–16 c–8a diffusion paths are three-dimensionally interconnected.<sup>16</sup> A schematic figure of the diffusion path is shown in Fig. 9. A major difference between the layered and spinel structure lies in the effect of the lattice parameter on the Li diffusivity. In layered materials such as  $\text{LiCoO}_2$ ,  $\text{LiNiO}_2$  and  $\text{LiNi}_{0.5}\text{Mn}_{1.5}\text{O}_2$ , the activation barrier for Li hopping depends very sensitively on the  $c$ -lattice parameter.<sup>44,60</sup> Any drop of the  $c$ -lattice parameter reduces the distance between the oxygen planes, and compresses the Li-slab space resulting in an increase in the activation barrier. In  $\text{Li}_x\text{CoO}_2$ , the decrease in  $c$ -lattice parameter as  $x < 0.4$  has a profound effect on the Li mobility<sup>61</sup> and limits the amount of capacity that can be achieved at reasonable rates. The  $\text{LiNi}_{0.5}\text{Mn}_{1.5}\text{O}_4$ , spinel on the other hand displays a high Li diffusivity throughout the full composition range. This may be because the activation energy for Li hopping depends less sensitively on the  $a$ -lattice parameter and the fact that the change in lattice parameter is smaller than that in the layered structure. The high Li diffusivity near the end of charge will enable complete access to the theoretical capacity of  $\text{LiNi}_{0.5}\text{Mn}_{1.5}\text{O}_4$ , spinel even at high rates.

## Conclusions

Nonstoichiometric  $\text{LiNi}_{0.5}\text{Mn}_{1.5}\text{O}_{4-\delta}$  thin-film cathodes have been prepared on stainless steel substrates by PLD. The XRD and SEM results show that the PLD film has a spinel structure with strong (111) texture, high crystallinity, and smooth surface. High capacity, excellent cycle performance, and good rate capability are obtained for cells made with these  $\text{LiNi}_{0.5}\text{Mn}_{1.5}\text{O}_{4-\delta}$  thin-film electrodes. The Li diffusivity of nonstoichiometric spinel  $\text{LiNi}_{0.5}\text{Mn}_{1.5}\text{O}_{4-\delta}$  is in the range of  $10^{-12}$  to  $10^{-10}$   $\text{cm}^2/\text{s}$  which is comparable to that of layered  $\text{LiCoO}_2$ . First principles calculations on the stoichiometric spinel  $\text{LiNi}_{0.5}\text{Mn}_{1.5}\text{O}_4$  find no intermediate phases between  $\text{LiNi}_{0.5}\text{Mn}_{1.5}\text{O}_4$  and  $\text{Li}_0\text{Ni}_{0.5}\text{Mn}_{1.5}\text{O}_4$ , indicating that the small step observed in experiments on ordered  $\text{LiNi}_{0.5}\text{Mn}_{1.5}\text{O}_4$  may be the result of partial disorder. Even though the chemical diffusion coefficient is maximal at  $x = 0.5$ , we find a minimum for the self-diffusion coefficient consistent with reduced vacancy mobility due to Li/vacancy ordering in the experimental samples. With

high Li diffusivity throughout almost all composition range,  $\text{LiNi}_{0.5}\text{Mn}_{1.5}\text{O}_{4-\delta}$  is a promising high-voltage cathode material for high-power applications.

### Acknowledgments

This research was supported by Advanced Materials for Micro- and Nano-System program under the Singapore-MIT Alliance and by the National University of Singapore. Y.S.M. and G.C. acknowledge the support by the Assistant Secretary for Energy Efficiency and Renewable Energy, Office of FreedomCAR and Vehicle Technologies of the U.S. Department of Energy under contract no. DE-AC03-76SF00098, via subcontracts no. 6517748 and 6517749 with the Lawrence Berkeley National Laboratory.

The Massachusetts Institute of Technology assisted in meeting the publication costs of this article.

### References

- J. M. Tarascon and D. Guyomard, *Electrochim. Acta*, **38**, 1221 (1993).
- D. Guyomard and J. M. Tarascon, *Solid State Ionics*, **69**, 222 (1994).
- H. Abiko, M. Hibino, and T. Kudo, *J. Power Sources*, **112**, 557 (2002).
- H. Kawai, M. Nagata, H. Kageyama, H. Takamoto, and A. R. West, *Electrochim. Acta*, **45**, 315 (1999).
- C. Sigala, D. Guyomard, A. Verbaere, Y. Piffard, and M. Tournoux, *Solid State Ionics*, **81**, 167 (1995).
- Q. Zhong, A. Bonakdarpour, M. Zhang, Y. Gao, and J. R. Dahn, *J. Electrochem. Soc.*, **144**, 205 (1997).
- H. Shigemura, H. Sakaebe, H. Kageyama, H. Kobayashi, A. R. West, R. Kanno, S. Morimoto, S. Nasu, and M. Tabuchi, *J. Electrochem. Soc.*, **148**, A730 (2001).
- Y. E. Eli, W. F. Howard, Jr., S. H. Lu, S. Mukerjee, J. Mcbreen, J. T. Vaughan, and M. M. Thackeray, *J. Electrochem. Soc.*, **145**, 1238 (1998).
- J. H. Kim, S. T. Myung, and Y. K. Sun, *Electrochim. Acta*, **49**, 219 (2004).
- S. H. Park and Y. K. Sun, *Electrochim. Acta*, **50**, 431 (2004).
- J. Reed and G. Ceder, *Chem. Rev. (Washington, D.C.)*, **104**, 4513 (2004).
- J. Reed, G. Ceder, and A. Van der Ven, *Electrochem. Solid-State Lett.*, **4**, A78 (2001).
- Z. H. Lu, L. Y. Beaulieu, R. A. Donabarger, C. L. Thomas, and J. R. Dahn, *J. Electrochem. Soc.*, **149**, A778 (2002).
- J. H. Kim, C. S. Yoon, S. T. Myung, J. Prakash, and Y. K. Sun, *Electrochem. Solid-State Lett.*, **7**, A216 (2004).
- J. H. Kim, S. T. Myung, C. S. Yoon, S. G. Kang, and Y. K. Sun, *Chem. Mater.*, **16**, 906 (2004).
- M. Wakihara, *Electrochemistry (Tokyo, Jpn.)*, **73**, 328 (2005).
- M. Kunduraci, J. F. Al-Sharab, and G. G. Amatucci, *Chem. Mater.*, **18**, 3585 (2006).
- B. Wang, J. B. Bates, F. X. Hart, B. C. Sales, R. A. Zuhr, and J. D. Robertson, *J. Electrochem. Soc.*, **143**, 3203 (1996).
- G. S. Chen, G. S. Chen, H. H. Hsiao, R. F. Louh, and C. J. Humphreys, *Electrochem. Solid-State Lett.*, **7**, A235 (2004).
- D. Singh, W. S. Kim, V. Craciun, H. Hofmann, and R. K. Singh, *Appl. Surf. Sci.*, **197-198**, 516 (2002).
- H. Xia, L. Lu, and G. Ceder, *J. Alloys Compd.*, **417**, 304 (2006).
- W. G. Choi and S. G. Yoon, *J. Power Sources*, **125**, 236 (2004).
- J. P. Maranchi, A. F. Hepp, and P. N. Kumta, *Mater. Sci. Eng., B*, **116**, 327 (2005).
- W. S. Yoon, S. H. Ban, K. K. Lee, K. B. Kim, M. G. Kim, and J. M. Lee, *J. Power Sources*, **97-98**, 282 (2001).
- M. Mohamedi, D. Takahashi, T. Itoh, M. Umeda, and I. Uchida, *J. Electrochem. Soc.*, **149**, A19 (2002).
- C. J. Wen, B. A. Boukamp, and R. A. Huggins, *J. Electrochem. Soc.*, **126**, 2258 (1979).
- P. E. Blochl, *Phys. Rev. B*, **50**, 17953 (1994).
- G. Kresse and J. Furthmuller, *Comput. Mater. Sci.*, **6**, 15 (1996).
- S. L. Dudarev, G. A. Botton, S. Y. Savrasov, C. J. Humphreys, and A. P. Sutton, *Phys. Rev. B*, **57**, 1505 (1998).
- F. Zhou, M. Cococcioni, C. A. Marianetti, D. Morgan, and G. Ceder, *Phys. Rev. B*, **70**, 235121 (2004).
- F. Zhou, C. A. Marianetti, M. Cococcioni, D. Morgan, and G. Ceder, *Phys. Rev. B*, **69**, 201101 (2004).
- M. K. Aydinol, A. F. Kohan, and G. Ceder, *J. Power Sources*, **68**, 664 (1997).
- H. Xia, S. B. Tang, L. Lu, Y. S. Meng, and G. Ceder, *Electrochim. Acta*, **52**, 2822 (2006).
- A. Van der Ven and G. Ceder, *Phys. Rev. B*, **59**, 742 (1999).
- A. Van der Ven, C. Marianetti, D. Morgan, and G. Ceder, *Solid State Ionics*, **135**, 21 (2000).
- Y. Terada, K. Yasaka, F. Nishikawa, T. Konishi, M. Yoshio, and I. Nakai, *J. Solid State Chem.*, **156**, 286 (2001).
- K. Dokko, M. Mohamedi, N. Anzue, T. Itoh, and I. Uchida, *J. Mater. Chem.*, **12**, 3688 (2002).
- C. Julien, E. Haro-Poniatowski, M. A. Camacho-Lopez, L. Escobar-Alarcon, and J. Jimenez-Jarquín, *Mater. Sci. Eng., B*, **72**, 36 (2000).
- Y. J. Park, J. G. Kim, M. K. Kim, H. G. Kim, H. T. Chung, and Y. Park, *J. Power Sources*, **87**, 69 (2000).
- B. Wang, J. B. Bates, F. X. Hart, B. C. Sales, R. A. Zuhr, and J. D. Robertson, *J. Electrochem. Soc.*, **143**, 3203 (1996).
- C. L. Liao and K. Z. Fung, *J. Power Sources*, **128**, 263 (2004).
- H. K. Kim and Y. S. Yoon, *J. Vac. Sci. Technol. A*, **22**, 1182 (2004).
- Y. I. Jang, N. J. Dudney, D. A. Blom, and L. F. Allard, *J. Power Sources*, **119-121**, 295 (2003).
- K. Kang, Y. S. Meng, J. Breger, C. P. Grey, and G. Ceder, *Science*, **311**, 977 (2006).
- H. Xia, L. Lu, and G. Ceder, *J. Power Sources*, **159**, 1422 (2006).
- K. M. Shaju and P. G. Bruce, *Adv. Mater. (Weinheim, Ger.)*, **18**, 2330 (2006).
- R. Amin, P. Balaya, and J. Maier, *Electrochem. Solid-State Lett.*, **10**, A13 (2007).
- D. Kovacheva, B. Markovsky, G. Salitra, Y. Talyosef, M. Gorova, E. Levi, M. Riboch, H. J. Kim, and D. Aurbach, *Electrochim. Acta*, **50**, 5553 (2005).
- M. Mohamedi, M. Makino, K. Dokko, T. Itoh, and I. Uchida, *Electrochim. Acta*, **48**, 79 (2002).
- T. Ohzuku, K. Ariyoshi, and S. Yamamoto, *J. Ceram. Soc. Jpn.*, **110**, 501 (2002).
- P. Strobel, A. Ibarra-Palos, M. Anne, C. Poinsignon, and A. Crisci, *Solid State Sciences*, **5**, 1009 (2003).
- K. Ariyoshi, Y. Iwakoshi, N. Nakayama, and T. Ohzuku, *J. Electrochem. Soc.*, **151**, A296 (2004).
- M. Kunduraci, J. F. Al-Sharab, and G. G. Amatucci, *J. Electrochem. Soc.*, **153**, A1357 (2006).
- Y. Gao, J. N. Reimers, and J. R. Dahn, *Phys. Rev. B*, **54**, 3878 (1996).
- A. Van der Ven and G. Ceder, *Solid State Ionics*, **135**, 21 (2000).
- B. Ammundsen, G. R. Burns, M. S. Islam, H. Kanoh, and J. Roziere, *J. Phys. Chem. B*, **103**, 5175 (1999).
- T. Kashiwagi, M. Nakayama, K. Watanabe, M. Wakihara, Y. Kobayashi, and H. Miyashiro, *J. Phys. Chem. B*, **110**, 4998 (2006).
- S. Buta, D. Morgan, A. Van der Ven, M. K. Aydinol, and G. Ceder, *J. Electrochem. Soc.*, **146**, 4335 (1999).
- A. Van der Ven and G. Ceder, *Electrochem. Solid-State Lett.*, **3**, 301 (2000).
- K. Kang and G. Ceder, *Phys. Rev. B*, **74**, 094105-1 (2006).
- H. Xia, L. Lu, Y. S. Meng, and G. Ceder, *J. Electrochem. Soc.*, **154**, A337 (2007).